

Revertant mutants G550E and 4RK rescue cystic fibrosis mutants in the first nucleotide-binding domain of CFTR by different mechanisms

Mónica Roxo-Rosa^{*†}, Zhe Xu[‡], André Schmidt^{*†}, Mário Neto^{*}, Zhiwei Cai[‡], Cláudio M. Soares[§], David N. Sheppard[‡], and Margarida D. Amaral^{*†¶}

^{*}Department of Chemistry and Biochemistry, Faculty of Sciences, University of Lisbon, Campo Grande, 1749-016 Lisbon, Portugal; [†]Centre of Human Genetics, National Institute of Health Dr. Ricardo Jorge, Avenida Padre Cruz, 1649-016 Lisbon, Portugal; [‡]Department of Physiology, School of Medical Sciences, University of Bristol, Bristol BS8 1TD, United Kingdom; and [§]Institute of Chemistry and Biological Technology, New University of Lisbon, 2781-901 Oeiras, Portugal

Communicated by Michael J. Welsh, University of Iowa College of Medicine, Iowa City, IA, September 22, 2006 (received for review June 9, 2006)

The revertant mutations G550E and 4RK [the simultaneous mutation of four arginine-framed tripeptides (AFTs): R29K, R516K, R555K, and R766K] rescue the cell surface expression and function of F508del-cystic fibrosis (CF) transmembrane conductance regulator (CFTR), the most common CF mutation. Here, we investigate their mechanism of action by using biochemical and functional assays to examine their effects on F508del and three CF mutations (R560T, A561E, and V562I) located within a conserved region of the first nucleotide-binding domain (NBD1) of CFTR. Like F508del, R560T and A561E disrupt CFTR trafficking. G550E rescued the trafficking defect of A561E but not that of R560T. Of note, the processing and function of V562I were equivalent to that of wild-type (wt)-CFTR, suggesting that V562I is not a disease-causing mutation. Biochemical studies revealed that 4RK generates higher steady-state levels of mature CFTR (band C) for wt- and V562I-CFTR than does G550E. Moreover, functional studies showed that the revertants rescue the gating defect of F508del-CFTR with different efficacies. 4RK modestly increased F508del-CFTR activity by prolonging channel openings, whereas G550E restored F508del-CFTR activity to wt levels by altering the duration of channel openings and closings. Thus, our data suggest that the revertants G550E and 4RK might rescue F508del-CFTR by distinct mechanisms. G550E likely alters the conformation of NBD1, whereas 4RK allows F508del-CFTR to escape endoplasmic reticulum retention/retrieval mediated by AFTs. We propose that AFTs might constitute a checkpoint for endoplasmic reticulum quality control.

endoplasmic reticulum quality control | folding | membrane traffic | arginine-framed motifs | trafficking signals

The common genetic disease cystic fibrosis (CF) is caused by mutations in the CF transmembrane conductance regulator (CFTR) (1). CFTR is a unique member of the ATP-binding cassette transporter superfamily that forms an epithelial anion channel with complex regulation (2, 3). It is composed of 1,480 amino acid residues organized into five domains: two membrane-spanning domains that form an anion-selective pore, two nucleotide-binding domains (NBDs) that likely form a head-to-tail dimer with two ATP-binding sites located at the dimer interface (4, 5), and a regulatory domain with multiple consensus phosphorylation sites (2).

CFTR biogenesis involves several steps that initiate with CFTR's synthesis in the endoplasmic reticulum (ER), where it is cotranslationally folded and core-glycosylated (6, 7). To undergo maturation through the Golgi apparatus, CFTR has to pass the ER quality control, which involves a number of chaperones and cochaperones (8–12), and targets misfolded proteins for ER-associated degradation by the ubiquitin proteasome pathway (13, 14). When correctly folded, CFTR is exported to the Golgi apparatus, where its N-linked glycan moiety undergoes further glycosylation to generate the mature fully glycosylated (processed) form of CFTR (15).

The most common CF mutation, occurring in at least one allele in 90% of patients, is the deletion of Phe-508 (F508del) of CFTR (1). The major impact of F508del is protein misfolding being the mutant recognized by the ER quality control, retained in the ER, and targeted for degradation by the proteasome (13, 16, 17). It is important to note that F508del-CFTR is a temperature-sensitive mutant that can be rescued by incubating cells that express it at reduced temperatures (18). However, when F508del-CFTR reaches the cell surface, its function is also found to be defective, e.g., channel gating (19) and regulation of other epithelial ion channels (20). Like low temperature, small molecules termed CFTR correctors (e.g., glycerol and bisaminomethylthiazoles) rescue the trafficking of F508del-CFTR to the cell surface (21, 22). Similarly, genetic factors (second-site mutations in cis with F508del) restore the cell surface localization of the mutant protein (23–26). DeCarvalho *et al.* (26) demonstrated that substitution of G550 by a negatively charged amino acid (G550E) promoted the maturation of F508del-CFTR and enhanced CFTR-mediated Cl⁻ permeability (26). Moreover, Chang *et al.* (25) rescued the trafficking and function of F508del-CFTR with the simultaneous mutation of the four arginine-framed tripeptides (AFTs) (R₂₉QR₃₁, R₅₁₆YR₅₁₈, R₅₅₃AR₅₅₅, and R₇₆₄RR₇₆₆) present in CFTR termed 4RK (R29K, R516K, R555K, and R766K). AFTs are transient retention/retrieval motifs coupling the ER export of multimeric membrane proteins to their folding/assembly (27).

Mechanistic insight into the different strategies that suppress the trafficking defect of F508del-CFTR is required for the development of effective therapies to correct the basic defect(s) in CF. To better understand how revertant mutants rescue F508del-CFTR, we selected for study the revertants G550E and 4RK for several reasons. First, they represent two very distinct types of amino acid residues (G550E, acidic; 4RK, basic). Second, they reside in distinct functional motifs (G550E, the LSGGQ motif of NBD1; 4RK, the AFTs). Third, they are likely to have different effects on the structure of CFTR because only two AFTs lie in NBD1 (like G550E), whereas the other two are on the N terminus and regulatory domain, respectively. Fourth, they have never before been expressed in the same cellular system and compared in parallel. Together, these reasons led us to hypothesize that G550E

Author contributions: M.R.-R. and Z.X. contributed equally to this work; D.N.S. and M.D.A. designed research; M.R.-R., Z.X., A.S., M.N., and C.M.S. performed research; Z.C. analyzed data; and M.R.-R., D.N.S., and M.D.A. wrote the paper.

The authors declare no conflict of interest.

Abbreviations: 4-PB, 4-phenylbutyrate; AFT, arginine-framed tripeptide; CF, cystic fibrosis; CFTR, CF transmembrane conductance regulator; ER, endoplasmic reticulum; IP, immunoprecipitation; IBI, interburst interval; MBD, mean burst duration; NBD, nucleotide-binding domain; WB, Western blot.

[¶]To whom correspondence should be addressed at: Faculty of Sciences, University of Lisbon, Campo Grande, C8 Building, 1749-016 Lisbon, Portugal. E-mail: mdamaral@fc.ul.pt.

© 2006 by The National Academy of Sciences of the USA

and 4RK act by different mechanisms. To explore this possibility, we tested the effects of G550E and 4RK on three additional CF mutations within NBD1: R560T, A561E, and V562I.^{||} We selected for study these CF mutants because (i) these residues constitute a hot spot for disease-causing mutations (seven mutations are associated with these three residues^{||}); (ii) A561E and R560T are the second and fourth most frequent mutations among Portuguese and Irish CF patients, respectively (28); (iii) like G550E and R555K (one of the 4RK mutants), these mutations affect residues located between the LSGGQ and Walker B motifs of NBD1, which are highly conserved across species; and (iv) they all lie within the same α -helix (H5; G550–Y563) within the ATP-binding cassette α -subdomain of NBD1 (29, 30). To test the hypothesis that G550E and 4RK act by different mechanisms, we used biochemical and functional assays to investigate how these revertants rescue F508del-, R560T-, A561E-, and V562I-CFTR.

Results

R560T, but Not V562I, Disrupts the Processing of CFTR. Like F508del-CFTR, many CF mutations disrupt the processing of CFTR and its delivery to the cell surface. Although revertants are known to rescue the cell surface expression of F508del-CFTR, their effects on other CF mutations in NBD1 is unknown. For the reasons outlined in the Introduction, we chose to analyze the CF mutations R560T, A561E, and V562I. Although we previously demonstrated that A561E is processed defectively (31), no trafficking data are available for mutations at R560 and V562. Therefore, we first investigated the processing of R560T and V562I by using Western blot (WB). Fig. 1A demonstrates that like F508del- and A561E-CFTR, R560T-CFTR generated only a discrete \approx 145 kDa band (band B). In contrast, band B and a diffuse \approx 180 kDa band (band C) were observed for both V562I-CFTR and wt-CFTR (Fig. 1A). These data suggest that R560T, disrupts the trafficking of CFTR, whereas V562I-CFTR is delivered to the cell surface.

Next, we investigated whether the revertants G550E and 4RK rescue the defective biosynthesis of R560T- and A561E-CFTR. As controls, the effects of the revertants on wt- and F508del-CFTR were tested. Fig. 1A shows that G550E and 4RK were much less effective at rescuing A561E-CFTR compared with their effects on F508del-CFTR. In fact, band C of both A561E-4RK- and A561E-G550E-CFTR was detected only after a 24 h incubation with 2 mM 4-phenylbutyrate (4-PB), an enhancer of CFTR expression through transcriptional activation (Fig. 1B) (32). Quantification of the data reveals that, after this treatment with 4-PB, \approx 30% of A561E-CFTR was rescued by either revertant, whereas for F508del-CFTR the value was \approx 65%. We confirmed the identity of these two bands as the core-glycosylated (immature) and fully glycosylated (mature) forms of CFTR by treating protein extracts with the glycosidases endoglycosidase H and *N*-glycanase F (Fig. 1C). These data indicate that the putative band B is the core-glycosylated form of CFTR present in the ER, whereas putative band C is the fully glycosylated form that has been processed through the Golgi apparatus.

We used CFTR immunoprecipitation (IP) after protein radiolabeling as a more sensitive approach to confirm our WB data in the absence of protein overexpression using 4-PB. The mature form of CFTR (band C) was clearly observed for F508del- and A561E-CFTR (Fig. 1D) in the presence of G550E and 4RK, but G550E failed to correct the defective biosynthesis of R560T-CFTR (Fig. 1A and D). Thus, the revertants G550E and 4RK rescue some, but not all, CF mutations in NBD1.

Effect of the G550E and 4RK Revertants on the Turnover and Processing of CFTR Variants. Fig. 1A demonstrates that steady-state levels of band C for both wt- and V562I-CFTR were increased by 4RK but not by G550E, most strikingly for V562I-CFTR. In contrast, the

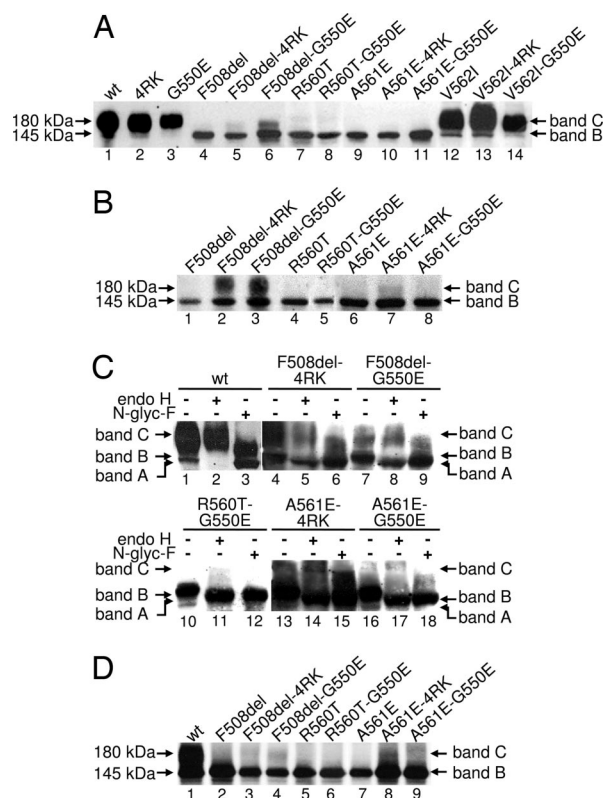


Fig. 1. Biochemical analysis of CFTR variants. (A) WB of total protein (30 μ g) from BHK cells stably expressing wt-, F508del-, R560T-, A561E-, or V562I-CFTR, alone or in cis with 4RK and G550E. (B) WB of samples as in A but after 24 h of incubation with 2 mM 4-PB to enhance protein expression. (C) Glycosidase analysis of total protein (250 μ g) extracts from BHK cells treated with 4-PB for 24 h. Protein extracts were treated with either 50 milliunits of endoglycosidase H (endo H) or 2 units of *N*-glycanase F (N-glyc F) before WB analysis. Minus and plus symbols denote the absence and presence of glycosidases, respectively. (D) BHK cells expressing F508del-, R560T-, or A561E-CFTR alone or in cis with the revertants 4RK and G550E were analyzed by CFTR IP after pulse-labeling for 3 h. Labeled arrows indicate the positions of bands A, B, and C.

revertants had the opposite effect on F508del-CFTR, with G550E generating higher steady-state levels of band C than 4RK (Fig. 1A). These data suggest that G550E and 4RK might alter the processing of CFTR in different ways. To investigate this, we examined the turnover rate of band B and the efficiency of its processing into band C for wt-, F508del- and V562I-CFTR alone or in cis with the revertants by pulse-chase analysis, followed by IP (Fig. 2A–C).

For wt-CFTR, the presence of the revertants, 4RK or G550E (dotted and dashed lines in Fig. 2D and G, respectively), did not alter either the turnover rate of band B (solid line in Fig. 2D) or the efficiency of its conversion into band C (compare dotted and dashed lines with solid line in Fig. 2G). Similarly, the turnover rate of band B of either F508del-4RK- or F508del-G550E-CFTR (dotted and dashed lines in Fig. 2E) was the same as that of F508del-CFTR (solid line, Fig. 2E). Moreover, Fig. 2H demonstrates identical processing efficiencies for F508del-4RK- and F508del-G550E-CFTR (compare the dotted and dashed lines). For V562I-CFTR, the turnover rate of V562I-G550E was slightly, but not significantly ($P > 0.05$), reduced compared with those of V562I- and V562I-4RK-CFTR (Fig. 2F). Furthermore, the efficiency of processing of V562I-4RK (dotted line, Fig. 2I) was slightly increased relative to those of V562I and V562I-G550E (solid and dashed lines, Fig. 2I, respectively). Finally, Fig. 2 shows that the turnover rates of V562I- and wt-CFTR were equivalent (slope of solid lines in D and F; $P > 0.05$), whereas the processing of V562I- was slightly faster than that of wt-CFTR (solid lines in G and I).

^{||}The CFTR Mutation Database: <http://www.sickkids.on.ca/cftr>.

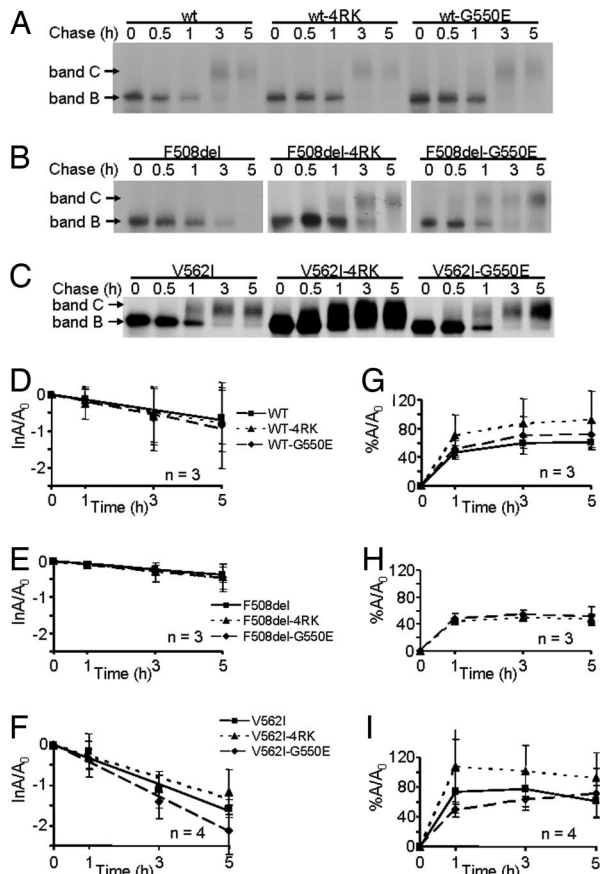


Fig. 2. Turnover and processing of wt-, F508del-, and V562I-CFTR alone or in cis with 4RK and G550E. (A–C) BHK cells expressing wt-, G550E- and 4RK-CFTR (A); F508del-, F508del-4RK-, and F508del-G550E-CFTR (B); and V562I-, V562I-4RK-, and V562I-G550E-CFTR (C) were pulse-labeled for 20 min with 100 $\mu\text{Ci/ml}$ [^{35}S]methionine and then chased for 0, 0.5, 1, 3, and 5 h. (D–F) Turnover of band B for wt- (D), F508del- (E), and V562I-CFTR (F) in the absence and presence of revertant mutations. Lines are the fit of first-order regressions to the data. Data are the natural logarithm of the amount of band B at a given time of chase (A) relative to its amount at the beginning of the experiment (A_0). (G and I) Efficiency of processing into band C for wt-CFTR (G) and V562I-CFTR (I) in the absence and presence of revertant mutations and for revertants of F508del-CFTR (H). Data are represented as the percentage of band C detected at a given time point during the experimental chase relative to A_0 . Symbols and error bars are means \pm SD of the values at each point.

Thus, the higher steady-state levels of band C for 4RK variants of both wt- and V562I-CFTR (Fig. 1A) are explained only in part by a slight (but not significant) increase in the efficiency of processing band B to band C. Surprised that the revertants did not exert stronger effects on the processing of CFTR, we wondered how they might influence CFTR Cl^- channel function.

WT- and V562I-CFTR Have Equivalent Functions. To begin to investigate the function of the CF mutants and revertants, we used the iodide (I^-) efflux technique, which assesses the function of a large population of CFTR Cl^- channels in intact cells. When cells expressing wt-CFTR were treated with the cAMP agonist forskolin (10 μM) and the CFTR potentiator genistein (50 μM), a robust efflux of I^- was elicited (Fig. 3A). Consistent with the biochemical data (Fig. 1), these agonists had no effect on F508del-, R560T-, or A561E-CFTR (Fig. 3B–D) but evoked a striking efflux of I^- from V562I-CFTR (Fig. 3E), which has a time course equivalent to that of wt-CFTR and 1.3-fold greater (Fig. 3F). A likely explanation for this enhanced efflux of I^- from V562I-CFTR-expressing cells is their greater membrane abundance of CFTR (Fig. 1A).

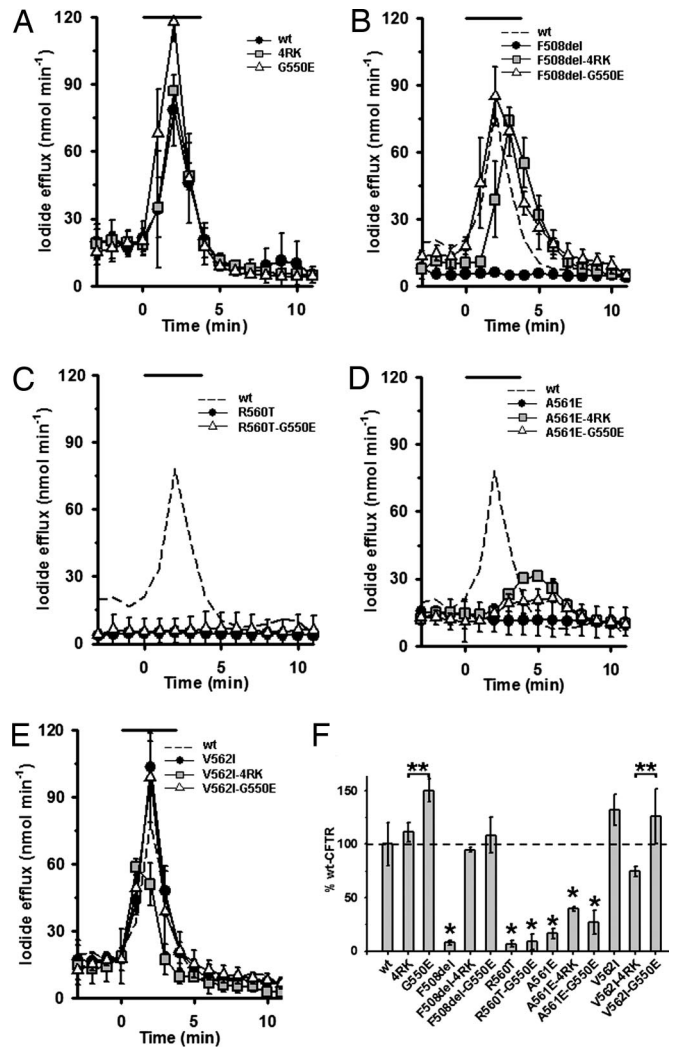


Fig. 3. Iodide efflux from cells expressing CFTR variants. (A–E) Time courses of I^- efflux from BHK cells stably expressing wt- (A), F508del- (B), R560T- (C), A561E- (D), and V562I- (E) CFTR in the absence and presence of the 4RK and G550E mutations. During the period indicated by the bars, 10 μM forskolin and 50 μM genistein were present in the efflux buffer. Data are means \pm SEM ($n = 4$) at each point. Where error bars are not shown, the symbol has obscured them. (F) Magnitude of peak I^- efflux generated by different CFTR constructs expressed as a percentage of that of wt-CFTR. Asterisks indicate values that are significantly different from wt-CFTR, and double asterisks refer to comparisons between the indicated pairs of data ($P < 0.05$).

Interestingly, the revertant 4RK, which generated higher steady-state levels of band C than wt-CFTR (Fig. 1A), produced an equivalent efflux of I^- to that of wt-CFTR (Fig. 3A and F). In contrast, G550E, which produced lower steady-state levels of band C than wt-CFTR (Fig. 1A), generated ≈ 1.5 -fold higher efflux of I^- (Fig. 3A and F). Consistent with previous work (24) and our biochemical data (Figs. 1 and 2), both 4RK and G550E restored CFTR function to F508del, although the time course of the F508del-4RK response was delayed by 1 min compared with that of wt-CFTR (Fig. 3B and F). In contrast to F508del-CFTR, G550E did not restore CFTR function to R560T and both revertants rescued only modestly the CFTR function of A561E (Fig. 3C, D, and F). Interestingly, V562I-G550E generated an efflux of I^- equivalent in magnitude and time-course to that of V562I-CFTR (Fig. 3E and F) despite its lower steady-state levels of band C. However, 4RK, which generated higher steady-state levels of band

C (Fig. 1A), decreased the magnitude of the V562I-evoked I⁻ efflux to a level equivalent to that of wt-CFTR (Fig. 3E and F).

Taken together, our iodide efflux data strongly suggest that the increased steady-state levels of band C (and the slight increase in CFTR processing efficiency) observed for the 4RK variants of wt- and V562I-CFTR (Figs. 1 and 2) do not result in increased CFTR channel activity. In contrast, the data suggest that G550E compensates for a decreased steady-state level of band C by enhancing the channel activity of wt- and V562I-CFTR. A similar mechanism might explain how G550E rescues the activity of CF mutants.

4RK and G550E Rescue F508del-CFTR Channel Gating with Different Efficacy. To test the idea that the revertant G550E enhances the Cl⁻ channel function of wt and CF mutants, we used the patch-clamp technique to study the single-channel behavior of wt-, V562I-, and F508del-CFTR in the absence and presence of the revertants. Fig. 4 demonstrates that the single-channel properties of V562I-CFTR were identical to those of wt-CFTR. Like wt-CFTR (2), the gating behavior of V562I-CFTR was characterized by bursts of channel openings interrupted by brief flickery closures and separated by longer closures between bursts (Fig. 4A). Strikingly, V562I-CFTR had the same open probability (P_o), mean burst duration (MBD), interburst interval (IBI), and ATP-dependence [V562I, ATP concentration for half maximal activation (K_m) = 252 μ M; wt, K_m = 210 μ M] as wt-CFTR (Fig. 4B–D and data not shown). Together with our observation that V562I-CFTR does not affect the efficiency of CFTR processing (Figs. 1 and 2), these data raise the possibility that V562I is not a disease-causing mutation.

Before examining the rescue of F508del-CFTR channel function by the revertants, we quantified the deficit in CFTR function caused by F508del and the effects of 4RK and G550E on wt-CFTR. Consistent with previous work (e.g., ref. 33), F508del severely perturbed CFTR channel gating, principally by diminishing the frequency of channel openings. F508del-CFTR attenuated MBD and dramatically prolonged IBI, with the result that its P_o was reduced markedly compared with that of wt-CFTR (Fig. 4B–D). The revertants 4RK and G550E enhanced wt-CFTR channel gating but with strikingly different efficacies. 4RK caused a small but not significant increase in P_o by lengthening MBD 2-fold, whereas G550E increased the P_o of wt-CFTR 1.5-fold by prolonging MBD 4.5-fold without altering IBI (Fig. 4B–D). Moreover, G550E dramatically enhanced the ATP-sensitivity of wt-CFTR (wt-CFTR, K_m = 210 μ M; G550E, K_m = 19 μ M; data not shown).

Like their effects on wt-CFTR, 4RK and G550E enhanced V562I-CFTR channel gating and rescued that of F508del-CFTR with different efficacies (Fig. 4). For example, Fig. 4A demonstrates that F508del-4RK- and F508del-G550E-CFTR both have prolonged channel openings compared with those of wt- and F508del-CFTR. But more strikingly, the IBI for F508del-G550E-CFTR is dramatically shorter than that of F508del-CFTR and approaches that of wt-CFTR (Fig. 4A). Fig. 4C demonstrates that both revertants prolonged strikingly the MBD of F508del-CFTR compared with that of either wt- or F508del-CFTR (4RK, 2.5-fold; G550E, 4-fold; both vs. F508del-CFTR). However, only G550E rescued the IBI defect of F508del-CFTR, reducing its IBI from 8-fold longer than wt-CFTR to only 2-fold longer (Fig. 4D). As a result, the P_o of F508del-G550E-CFTR exceeded that of wt-CFTR, whereas that of F508del-4RK is only half that of wt-CFTR (Fig. 4B). To summarize, our data demonstrate that the revertant G550E efficaciously rescues the gating defect of F508del-CFTR, whereas rescue by 4RK is modest. We interpret these data to suggest that 4RK and G550E exert their effects on F508del by different mechanisms.

Discussion

R560, A561, and V562 constitute a hot spot for mutations within a conserved region of NBD1 located between the LSGGQ and Walker B motifs. Like F508del, R560T and A561E disrupt CFTR

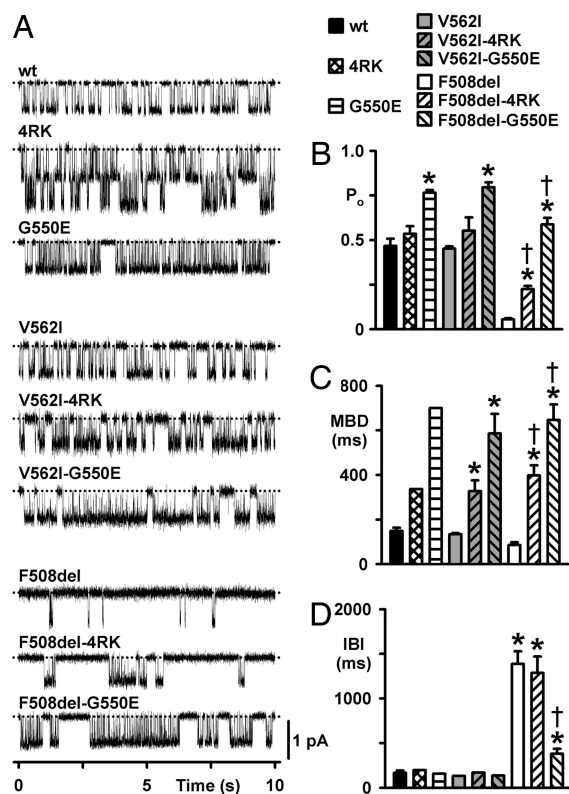


Fig. 4. Single-channel activity of wt-, V562I-, and F508del-CFTR alone and in cis with 4RK and G550E. (A) Representative single-channel recordings of the indicated mutants in excised inside-out membrane patches (see *Methods*). Dotted lines indicate the closed channel state, and downward deflections correspond to channel openings. (B–D) P_o (B), MBD (C), and IBI (D) of the indicated CFTR variants. Columns and error bars are means \pm SEM (wt: n = 6 for all data; 4RK: P_o , n = 2; MBD and IBI, n = 1; G550E: P_o , n = 3; MBD and IBI, n = 1; V562I: P_o , n = 5; MBD and IBI, n = 2; V562I-4RK: P_o , n = 4; MBD and IBI, n = 3; V562I-G550E: P_o , n = 8; MBD and IBI, n = 3; F508del: n = 10 for all data; F508del-4RK: P_o , n = 13; MBD and IBI, n = 10; F508del-G550E: P_o , n = 5; MBD and IBI, n = 4). Asterisks indicate values that are significantly different from that of wt-CFTR (P < 0.001); daggers indicate values significantly different from F508del-CFTR (P < 0.001). For wt- and F508del-CFTR, C127 cells expressing these variants were used to determine values of P_o , MBD, and IBI, but the single-channel traces shown in A are all from BHK cells expressing the indicated variants. In two single-channel patches from BHK cells expressing wt- and F508del-CFTR values of i and P_o did not differ from those of C127 cells expressing these variants (data not shown).

processing, whereas V562I traffics normally to the cell surface, forming a Cl⁻ channel with properties indistinguishable from those of wt-CFTR. The revertants 4RK and G550E rescue the cell surface expression of A561E, albeit not as effectively as F508del, whereas G550E is without effect on R560T. Of note, G550E, but not 4RK, rescues the defective channel gating of F508del, suggesting that G550E and 4RK rescue the expression and function of F508del by distinct mechanisms.

To understand the structural basis by which R560T and A561E disrupt the processing of CFTR (refs. 31 and 34 and present results), we generated a comparative model of the human NBD1-NBD2 dimer (data not shown). In our model and the crystal structure of human NBD1 (30), the side chain of R560 is partially buried in the tertiary structure of NBD1. R560T likely disrupts the interactions of R560 with neighboring residues and, hence, the folding of NBD1. The fact that other CF-causing mutations at R560 (e.g., R560G) also cause severe disease highlights the importance of this residue for the global structure of CFTR. Similarly, A561 is partially buried in the tertiary structure of NBD1, suggesting that changing this residue also causes NBD1 misfolding.

Surprisingly, our data demonstrate that V562I-CFTR is processed as efficiently as wt-CFTR (Fig. 2) and forms a Cl⁻ channel functionally equivalent to wt-CFTR (Fig. 4). Indeed, our structural model predicts that V562I is without effect on the tertiary structure of NBD1. Based on these data, we do not consider V562I-CFTR to be a CF-causing variant. Consistent with this idea, this mutation was originally reported to be a sequence polymorphism. Moreover, two individuals with the F508del/V562I genotype have no clinical signs of CF (C. Barreto, personal communication).

Structural studies of human NBD1 suggest that the deletion of F508 *per se* does not have a major impact on the stability or folding of NBD1, given its local surface topography (29, 30). Moreover, F508del is predicted to be without major effect on the structure of the NBD1–NBD2 dimer because it lies far from its interface. Thus, it was suggested that the absence of F508 should impair the kinetics of either cotranslational folding or interdomain folding (9, 35–38).

However, it remains possible that deletion of F508 causes intrinsic misfolding and/or structural instability of NBD1 at steady state (39, 40). Supporting this idea, the F508del-CFTR Cl⁻ channel has a gating defect characterized by a reduction in the duration of channel openings and a dramatic prolongation of periods when the channel is closed. By using the ATP-dependent dimerization model of CFTR channel gating (4), the exceptionally slow rate of channel opening might be explained by F508del inducing misfolding and/or structural instability of NBD1, which would hamper ATP binding. Similarly, the reduced open time of F508del might result from the mutation weakening the binding energy for stable NBD1–NBD2 dimer formation. However, because NBD1 α -helices involved in the dimer interface lie opposite the F508 residue (29, 30), this explanation is hard to accept unless some distortion of NBD1 occurs. Alternatively, F508del might alter the packing of NBD1 with the membrane-spanning domains (30) without causing major NBD1 misfolding.

If functional data suggest that F508del perturbs the structure of NBD1, why, then, were only minimal changes observed in the crystal structure of F508del-NBD1 (30)? Significantly, the crystal structure of F508del-NBD1 contains a number of solubilizing mutations. Perhaps the presence of these mutations abrogates the impact of F508del on the structure of NBD1. Consistent with this idea, Hegedus *et al.* (40) recently suggested that F508del causes steady-state structural instability. Alternatively, or in addition, F508del might alter the dynamic properties of CFTR, a possibility that would remain imperceptible in the crystal structure of NBD1.

DeCarvalho *et al.* (26) identified the revertant G550E by using STE6/CFTR chimeras to search for F508del suppressor mutations. The authors demonstrated that G550E (*i*) partially rescues the processing defect of F508del-CFTR, (*ii*) enhances F508del-CFTR Cl⁻ currents in Fischer rat thyroid (FRT) epithelia, and (*iii*) increases the sensitivity of F508del-CFTR to stimulation by cAMP agonists (26). Our own biochemical and functional data concur with these data. Any difference in the level of F508del rescue between previous studies of 4RK (25) and G550E (26) and our own are most likely due to the use of different cell lines. Of note, our single-channel data provide an explanation for the effects of G550E on F508del-CFTR activity. The revertant accelerated dramatically the rate of channel openings and slowed markedly the rate of channel closing. This suggests that G550E might promote the binding of ATP to site 1 of the NBD dimer while slowing the hydrolysis of ATP at site 2, plausibly by stabilizing the NBD dimer (4). Thus, we speculate that the gating behavior of F508del-G550E-CFTR might be a consequence of a (partial) correction the F508del-induced folding defect of NBD1.

The cellular machinery responsible for recognition of AFT signals remains poorly characterized. AFTs were demonstrated to behave as protein ER-retention signals with no requirements other than sufficient exposure (27). Interestingly, some membrane proteins with exposed AFTs exit the ER to pre-Golgi compartments but then are retrieved to the ER by a COPI (coat protein complex

I)-mediated process (27, 41). This finding suggests that the four AFTs in CFTR are buried within the protein when CFTR is in its native conformation. When CFTR becomes misfolded, these AFTs are exposed, becoming targets for ER retention/retrieval (25). Removal of AFTs likely uncouples ER export from protein folding by making proteins invisible to the retention/retrieval machinery (27). This explains the observed rescue of the cell surface expression of F508del- and A561E-CFTR by the 4RK revertant. However, such an explanation does not imply correction of the folding defects of F508del- and A561E-CFTR. Consistent with this idea, our single-channel data demonstrate that 4RK incompletely rescues the gating defect of F508del-CFTR, unlike the G550E revertant.

Jurkuvenaite *et al.* (42) recently studied R31C and R31L, two CF mutations in the N terminus of CFTR that affect the first AFT (R₂₉QR₃₁). Their data demonstrate enhanced internalization from the cell surface, which suggests that some of the reduction in the steady-state levels of band C that we observed with F508del-4RK-CFTR might be explained by enhanced internalization. However, the opposite effect was observed for both wt- and V562I-CFTR when in cis with 4RK; therefore, the effects observed with the R31 mutants must result from the loss of a stabilizing role played by the N terminus rather than from interference with an AFT.

Recent work (4) suggests that R555, one of the four AFT in CFTR, plays a critical role in the formation of the NBD1–NBD2 dimer. However, earlier work by Teem *et al.* (24) demonstrated that mutation of R555 by itself acts as a F508del-CFTR revertant, not just by rescuing its cell surface expression, but also by enhancing channel gating. Interestingly, different patterns of channel gating have been reported for R555K-CFTR. Teem *et al.* (24) demonstrated that R555K increases the activity of wt-CFTR by extending the duration of bursts without altering the closed time interval between bursts. In contrast, Vergani *et al.* (4) showed that R555K slows the rate of channel opening by markedly prolonging the closed time interval between bursts. A likely explanation for these differences in channel gating is the experimental conditions used. Teem *et al.* (24) studied CFTR channel gating at 37°C, whereas Vergani *et al.* (4) used room temperature. Of note, the work of Hegedus *et al.* (40), who studied F508del-CFTR in cis with R29K and R555K (called 2RK), suggests that the stability of F508del-2RK-CFTR is temperature-dependent. They demonstrated that 2RK restored F508del-CFTR activity to values similar to those of wt-CFTR at 30°C but not at higher temperatures (40). Hegedus *et al.* (40) observed that 2RK has reduced resistance to proteolysis compared with that of wt-CFTR and speculated that this occurs because F508del-2RK-CFTR adopts a less compact conformation. Thus, it appears that the partially misfolded form of F508del-4RK-CFTR [or F508del-2RK-CFTR (40)] is able to escape rapid ER-associated degradation and the ER quality control checkpoints of the Hsp70 machinery and calnexin (12) and traffic out of the ER. Then, because of the absence of AFTs, this ER-exported but still partially misfolded CFTR is processed through the Golgi apparatus and trafficked to the plasma membrane, where it still exhibits a defect in channel gating. Thus, we propose that besides the two previously described ER folding checkpoints (12), there is a third AFT-mediated retention/retrieval checkpoint at the ER/early Golgi apparatus that monitors the folding status of CFTR en route to the cell surface.

In summary, our studies indicate that the location of CF mutations within the H5 α -helix of NBD1 determines the efficacy with which the revertants G550E and 4RK restore their function: Mutations located proximally are rescued better than those located distally. This suggests that the H5 α -helix plays a critical role in the structure and function of CFTR. Moreover, our data demonstrate that the revertants 4RK and G550E produce distinct effects on F508del-CFTR: 4RK affects mainly the efficiency of processing, enabling the mutant to escape AFT-mediated ER retention/retrieval, with only limited rescuing of folding. In contrast, G550E

appears to exert its effect directly on the conformation of NBD1, as it rescues efficaciously the gating defect of F508del-CFTR. Because G550 lies within NBD1, we consider that its correction of the F508del gating defect likely represents the correction of an existing F508del-NBD1 conformational defect and, hence, the stabilization of the conformation of NBD1 and/or the global structure of CFTR.

Methods

Site-Directed Mutagenesis, Cells, and CFTR Expression. By using the QuikChange mutagenesis kit (Stratagene, La Jolla, CA), we introduced mutations into CFTR in the pNUT vector (12, 45). We transfected BHK cells with 2 μ g of each CFTR variant by using Lipofectin (Invitrogen, Carlsbad, CA) and selected for stable transfectants by using 500 μ M methotrexate. After 10 days, individual clones were isolated and assessed for CFTR expression by WBs. When compared with both wt- and F508del-CFTR, clones expressing V562I- and R560T-CFTR expressed higher and lower levels of protein, respectively, precluding studies on cell lines with equivalent amounts of CFTR protein. For biochemical and I⁻ efflux assays, we seeded cells onto 60-mm Petri dishes and used them 2–3 days later, whereas, for patch-clamp studies, cells were seeded onto glass coverslips and used 2–5 days later. In some experiments, CFTR expression was enhanced by either incubating cells with 2 mM 4-PB for 24 h or at 26°C for 72 h.

Western Blotting, Metabolic Labeling, and CFTR IP. For WB, cells were lysed, and 30 μ g of total protein was analyzed as described (10, 43) by using the anti-CFTR monoclonal antibody M3A7 (Chemicon, Temecula, CA) to detect specifically CFTR and the SuperSignal West Pico chemiluminescent substrate system (Pierce, Rockford, IL) to develop WBs. For metabolic labeling, cells (\approx 70% confluent) were starved for 30 min in methionine-free MEM (Invitrogen) before being radiolabeled for 20 min in the same medium supplemented with 100 μ Ci/ml [³⁵S]methionine (1 Ci = 37 GBq) (ICN Biomedicals, Irvine, CA). For the chase (0, 0.5, 1, 3, and 5 h), the labeling medium was replaced by MEM with 5% (vol/vol) FBS and 1 mM nonradioactive methionine. CFTR IP, electrophoresis, fluorography, and densitometry were performed as described (10).

Glycosidase Assays. We treated total protein extracts from BHK cell lines expressing CFTR variants with glycosidases as described (43). In brief, 250 μ g of total protein extracts were incubated with 50 milliunits of endoglycosidase H (Genzyme, Cambridge, MA) for 18 h at 37°C in the appropriate buffer or with 2 units of N-glycanase F (Roche, Basel, Switzerland) for 18 h at 37°C. After protein precipitation, samples were subjected to WB.

Iodide Efflux. Experiments were performed as described previously (44) by using fully confluent dishes of cells and with 10 μ M forskolin and 50 μ M genistein. The amount of I⁻ was determined by an I⁻-selective electrode (ThermoElectron Corporation, Waltham, MA).

Electrophysiology. CFTR Cl⁻ channels were recorded in excised inside-out membrane patches by using an Axopatch 200A patch-clamp amplifier (Molecular Devices, Union City, CA) and pCLAMP data acquisition and analysis software (versions 6.03 and 9.0.0; Molecular Devices), as described (44). To activate and sustain channel activity, 75 nM PKA and 1 mM ATP were added to all intracellular solutions; voltage was clamped at -50 mV. For single-channel studies, we used membrane patches containing \leq 5 active channels, determining the number of active channels based on the maximum number of simultaneous channel openings (45).

Statistics. Results are expressed as means \pm SEM of *n* observations. Pulse-chase data were analyzed as described (10). To test for differences, either a one-way ANOVA followed by the Dunnett T3 post hoc test or a Student *t* test was used. Differences were considered statistically significant when *P* < 0.05. Tests were performed by using SigmaStat (version 2.03; Jandel Scientific, Erkrath, Germany).

We thank Paulo Nogueira for assistance with statistics. This work was supported by Grants POCTI/MGI/47382/2002 and POCTI/SAU/MMO/58425/2004 from the Foundation for Science and Technology (Portugal) and the European Union, pluriannual funding from the Centro de Investigação em Genética Molecular Humana (Portugal), and the Cystic Fibrosis Trust (United Kingdom). M.R.-R. and A.S. were recipients of Praxis Ph.D. Fellowships BD/19869/99 and SFRH/BD/19415/2004, respectively. Z.X. is supported by the University of Bristol and an award from the Overseas Research Students Award Scheme.

1. Welsh MJ, Ramsey BW, Accurso FJ, Cutting GR (2001) in *The Metabolic Basis of Inherited Disease*, eds. Scriver CR, Beaudet AL, Sly WS, Valle D (McGraw-Hill, New York), pp 5121–5188.
2. Sheppard DN, Welsh MJ (1999) *Physiol Rev* 79:S23–S45.
3. Riordan JR (2005) *Annu Rev Physiol* 67:701–718.
4. Vergani P, Lockless SW, Nairn AC, Gadsby DC (2005) *Nature* 433:876–880.
5. Moran O, Galiotta LJ, Zegarra-Moran O (2005) *Cell Mol Life Sci* 62:446–460.
6. Lu Y, Xiong X, Helm A, Kimani K, Bragin A, Skach WR (1998) *J Biol Chem* 273:568–576.
7. Kleizen B, van Vlijmen T, de Jonge HR, Braakman I (2005) *Mol Cell* 20:277–287.
8. Loo MA, Jensen TJ, Cui L, Hou Y, Chang XB, Riordan JR (1998) *EMBO J* 17:6879–6887.
9. Meacham GC, Lu Z, King S, Sorscher E, Tousson A, Cyr DM (1999) *EMBO J* 18:1492–1505.
10. Farinha CM, Nogueira P, Mendes F, Penque D, Amaral MD (2002) *Biochem J* 366:797–806.
11. Meacham GC, Patterson C, Zhang W, Younger JM, Cyr DM (2001) *Nat Cell Biol* 3:100–105.
12. Farinha CM, Amaral MD (2005) *Mol Cell Biol* 25:5242–5252.
13. Ward CL, Omura S, Kopito RR (1995) *Cell* 83:121–127.
14. Jensen TJ, Loo MA, Pind S, Williams DB, Goldberg AL, Riordan JR (1995) *Cell* 83:129–135.
15. Amaral MD (2004) *J Mol Neurosci* 23:41–48.
16. Cheng SH, Gregory RJ, Marshall J, Paul S, Souza DW, White GA, O’Riordan CR, Smith AE (1990) *Cell* 63:827–834.
17. Lukacs GL, Mohamed A, Kartner N, Chang XB, Riordan JR, Grinstein S (1994) *EMBO J* 13:6076–6086.
18. Denning GM, Anderson MP, Amara JF, Marshall J, Smith AE, Welsh MJ (1992) *Nature* 358:761–764.
19. Dalemans W, Barbry P, Champigny G, Jallat S, Dott K, Dreyer D, Crystal RG, Pavirani A, Lecocq JP, Lazdunski M (1991) *Nature* 354:526–528.
20. Kunzelmann K (2001) *News Physiol Sci* 16:167–170.
21. Brown CR, Hong-Brown LQ, Biwersi J, Verkman AS, Welch WJ (1996) *Cell Stress Chaperones* 1:117–125.
22. Pedemonte N, Lukacs GL, Du K, Caci E, Zegarra-Moran O, Galiotta LJ, Verkman AS (2005) *J Clin Invest* 115:2564–2571.
23. Teem JL, Berger HA, Ostedgaard LS, Rich DP, Tsui LC, Welsh MJ (1993) *Cell* 73:335–346.
24. Teem JL, Carson MR, Welsh MJ (1996) *Recept Channels* 4:63–72.
25. Chang XB, Cui L, Hou YX, Jensen TJ, Aleksandrov AA, Mengos A, Riordan JR (1999) *Mol Cell* 4:137–142.
26. DeCarvalho AC, Gansheroff LJ, Teem JL (2002) *J Biol Chem* 277:35896–35905.
27. Michelsen K, Yuan H, Schwappach B (2005) *EMBO Rep* 6:717–722.
28. World Health Organization (2004) *The Molecular Genetic Epidemiology of Cystic Fibrosis: Report of a Joint Meeting of WHO/ECFTN/ICF(MA)/ECFS* (WHO, Geneva).
29. Lewis HA, Buchanan SG, Burley SK, Connors K, Dickey M, Dorwart M, Fowler R, Gao X, Guggino WB, Hendrickson WA, et al. (2004) *EMBO J* 23:282–293.
30. Lewis HA, Zhao X, Wang C, Sauder JM, Rooney I, Noland BW, Lorimer D, Kearns MC, Connors K, Condon B et al. (2005) *J Biol Chem* 280:1346–1353.
31. Mendes F, Roxo-Rosa M, Dragomir A, Farinha CM, Roomans GM, Amaral MD, Penque D (2003) *Biochem Biophys Res Commun* 311:665–671.
32. Roth SY, Denu JM, Allis CD (2001) *Annu Rev Biochem* 70:81–120.
33. Haws CM, Nepomuceno IB, Krouse ME, Wakelee H, Law T, Xia Y, Nguyen H, Wine JJ (1996) *Am J Physiol* 270:C1544–C1555.
34. Champigny G, Imler JL, Puchelle E, Dalemans W, Gribkoff V, Hinrasky J, Dott K, Barbry P, Pavirani A, Lazdunski M (1995) *EMBO J* 14:2417–2423.
35. Qu BH, Strickland E, Thomas PJ (1997) *J Bionerg Biomembr* 29:483–490.
36. Qu BH, Strickland EH, Thomas PJ (1997) *J Biol Chem* 272:15739–15744.
37. Chen EY, Bartlett MC, Loo TW, Clarke DM (2004) *J Biol Chem* 279:39620–39627.
38. Du K, Sharma M, Lukacs GL (2005) *Nat Struct Mol Biol* 12:17–25.
39. Sharma M, Benharouga M, Hu W, Lukacs GL (2001) *J Biol Chem* 276:8942–8950.
40. Hegedus T, Aleksandrov A, Cui L, Gentsch M, Chang XB, Riordan JR (2006) *Biochim Biophys Acta*, 1758:563–572.
41. Nufer O, Hauri HP (2003) *Curr Biol* 13:R391–R393.
42. Jurkuvenaite A, Varga K, Nowotarski K, Kirk KL, Sorscher EJ, Li Y, Clancy JP, Bebek Z, Collawn JF (2006) *J Biol Chem* 281:3329–3334.
43. Farinha CM, Penque D, Roxo-Rosa M, Lukacs G, Dormer R, McPherson M, Pereira M, Bot AG, Jorna H, Willemsen R, et al. (2004) *J Cyst Fibros* 3(Suppl 2):73–77.
44. Lansdell KA, Kidd JF, Delaney SJ, Wainwright BJ, Sheppard DN (1998) *J Physiol* 512:751–764.
45. Cai Z, Scott-Ward TS, Sheppard DN (2003) *J Gen Physiol* 122:605–620.